

Single Crystal, High Band Gap CdS Thin Films Grown by RF Magnetron Sputtering in Argon Atmosphere for Solar Cell Applications

Rupali Kulkarni¹, Amit Pawbake¹, Ravindra Waykar¹, Ashok Jadhavar¹, Haribhau Borate¹, Rahul Aher¹, Ajinkya Bhorde¹, Shruthi Nair¹, Priyanka Sharma¹, Sandesh Jadkar^{2*}

¹ School of Energy Studies, Savitribai Phule Pune University, 411 007 Pune, India

² Department of Physics, Savitribai Phule Pune University, 411 007 Pune, India

(Received 01 March 2018; revised manuscript received 09 June 2018; published online 25 June 2018)

Single crystal thin films of CdS were grown onto glass substrates by RF magnetron sputtering at various substrate temperatures. Structural, optical and morphology properties of these films were investigated through low angle XRD, Raman spectroscopy, scanning electron microscopy (SEM), energy dispersive x-ray (EDX) spectroscopy, UV-Visible spectroscopy etc. Formation of single crystal CdS films has been confirmed by low angle XRD and Raman spectroscopy analysis. Low angle XRD showed that CdS films has preferred orientation in (111) direction. Improvement of crystallinity and increase in average grain size of CdS crystallites has been observed with increase in substrate temperature. Surface morphology investigated using SEM showed that CdS films deposited over entire range of substrate temperature are highly smooth, dense, homogeneous, and free of flaws and cracks. The EDX data revealed the formation of high-quality nearly stoichiometric CdS films by RF magnetron sputtering. Furthermore, the CdS films deposited at low substrate temperatures (< 200 °C) are slightly S rich while deposited at higher substrate temperatures (> 200 °C) are slightly Cd rich. The UV-Visible spectroscopy analysis showed that an average transmission ~ 80-90 % in the visible range of the spectrum having band gap ~ 2.28 -2.38 eV, which is quite close to the optimum value of band gap for a buffer layer in CdTe/CdS, Cu₂S/CdS hetero-junction solar cells.

Keywords: CdS films, RF magnetron sputtering, Low angle XRD, Raman spectroscopy, EDX spectroscopy.

DOI: [10.21272/jnep.10\(3\).03005](https://doi.org/10.21272/jnep.10(3).03005)

PACS numbers: 81.15.Cd, 81.07.Bc

1. INTRODUCTION

Thin films technology is the most promising technology for mass production of solar cells due to the low cost solar energy conversion, low materials consumption and the possibility to obtain very small integrated solar cell modules. Cadmium sulphide (CdS) belonging to the II-VI group received considerable attention in recent years for thin film solar cell applications due to its excellent properties such as wide and direct band gap (~ 2.42 eV) at room temperature, high carrier concentration (~ 10¹⁶ cm⁻³), mobility (~ 5 cm² V⁻¹ s⁻¹) [1], high absorption coefficient (~ 10⁴ cm⁻¹), high electrochemical stability [2] etc. As per as solar cells are concerned, CdS has been used as a window material together with several semiconductors such as copper indium gallium selenide (CIGS), copper zinc tin sulfide (CZTS), cadmium telluride (CdTe), copper sulfide (Cu₂S) based solar cells [3].

There are several deposition techniques used for the deposition of CdS thin films. These includes vacuum evaporation [4], flash evaporation [5], molecular beam epitaxy (MBE) [6], sputtering [7] and screen printing [8], pulsed laser ablation (PLA) [9], electrodeposition [10], successive ionic layer adsorption and reaction (SILAR) [11], chemical bath deposition (CBD) [12], chemical spray pyrolysis (CSP) [13], close space sublimation (CSS) [14], chemical vapor deposition [15] etc. Each deposition method has its own advantages and limitations and each deposition process produces different structural, electrical, optical and morphology properties of the CdS thin films. Considering the high material utilization ratio, availability of existing sophisticated

facilities and possibility of scaling up for large area deposition sputtering has been established for industrial applications. Furthermore, the RF magnetron sputtering permits deposition at low temperature, and gives better adhesion, larger coverage and higher film density than other methods.

The physical properties of CdS thin films deposited by RF magnetron sputtering method are affected by the deposition parameters such as sputtering power, argon gas pressure, substrate temperature, target-substrate distance etc. However, the relation between the variation of deposition parameter and the resulting film properties has not been yet fully established. So far, there exist few reports on investigation of substrate temperature dependent properties of CdS thin films prepared by using RF magnetron sputtering method [16, 17]. It is with this motivation an attempt has been made to study the synthesis and characterization of CdS thin films using RF magnetron sputtering method. In this paper, we report detail investigation of influence of substrate temperature on structural, optical, morphology and compositional properties of CdS thin films deposited by RF magnetron sputtering method.

2. EXPERIMENTAL

2.1. Preparation of Films

The CdS films were deposited on corning #7059 substrates using home-built RF magnetron sputtering system details of which been described elsewhere [18]. It consists of a cylindrical stainless steel chamber (process chamber) coupled with a turbo molecular pump

* sandesh@physics.unipune.ac.in

(TMP) followed by a roughing pump which yields a base pressure less than 10^{-7} Torr. A target of 4 inch diameter (99.99 %, Vin Karola Instrument, USA) was used for the deposition of CdS films and was kept facing the substrate holder ~ 7 cm away. To ensure the uniformity of films substrates were kept rotating during the sputtering process using a stepper motor with variable speed. The substrates can be clamped on substrate holder which is heated by inbuilt heater using thermocouple and temperature controller. The substrate temperature was varied from 50°C to 400°C . The pressure during deposition was kept constant by using automated throttle valve and measured with capacitance manometer. Sputtering gas, argon (Ar) can be introduced in the process chamber through a specially designed gas bank assembly which consist of mass flow controllers (MFCs) and gas mixing. The process parameters employed during the deposition of CdS films are listed in Table 1.

Table 1 – Process parameters employed during the deposition of CdS films

Process parameter	Value
Deposition pressure (p_{dep})	5×10^{-3} mbar
Deposition time (t)	30 min
RF power (P_{RF})	100 W
Target-to-substrate distance (d_{t-s})	7 cm
Ar gas flow rate (F_{Ar})	30 sccm
Substrate temperature (T_{Sub})	$50\text{-}400^\circ\text{C}$

The substrates were cleaned using a standard cleaning procedure. Prior to each deposition, the substrate holder and deposition chamber were baked for two hours at 100°C to remove any water vapor absorbed on the substrates and to reduce the oxygen contamination in the film. After that, the substrate temperature was brought to desired value by appropriately setting the inbuilt thermocouple and temperature controller. Sputter-etch of 10 min were used to remove the target surface contamination. The deposition was carried out for desired amount of time and films were allowed to cool to room temperature in vacuum.

2.2 Characterization of Films

Low angle X-ray diffraction pattern was obtained by x-ray diffractometer (Bruker D8 Advance, Germany) using $\text{CuK}\alpha$ line ($\lambda = 1.54056 \text{ \AA}$) at a grazing angle of 1° . The average crystallite size was estimated using the classical Scherrer's formula. The band gap of the films was deduced from transmittance and reflectance spectra of the films deposited on corning glass using a JASCO, V-670 UV-Visible spectrophotometer in the range 350-800 nm by using the procedure followed by Tauc. Raman spectra were recorded with Raman spectrophotometer (Jobin Yvon Horibra LABRAM-HR) in the range $200\text{-}800 \text{ cm}^{-1}$. The spectrometer has backscattering geometry for detection of Raman spectrum with the resolution of 1 cm^{-1} . The excitation source was 532 nm line of He-Ne laser. The power of the Raman laser was kept less than 5 mW to avoid laser-induced crystallization of the films. The scanning electron microscopy (SEM) images were recorded using a JEOL JSM-6360A microscope with operating voltage

20 kV to study the surface morphology of the films. The thickness of films was determined by a profilometer (KLA-Tencor, P-16+).

3. RESULTS AND DISCUSSION

Sputtering is momentum exchange phenomenon between ion and atom of the target material. Sputtering simply means ejection of electron from its solid material (target) due to bombardment of energetic particles (which are normally gas molecules). The kinetic energy of the bombarding particle is much greater than conventional thermal energy. In RF magnetron sputtering method for deposition of thin films change in the substrate temperature changes the opto-electronic properties of films through changes in its structure and composition. An increase in substrate temperature increases the energy for the surface mobility for the film precursors, it increases their diffusion length and therefore proper relaxation of the film structure during the film growth is possible. However increase in substrate temperature can have some adverse effect on the film properties too. A balance between the beneficial and the adverse effects of increase in substrate temperature at a particular temperature range results in a device quality film structure.

3.1 Variation of Film Thickness

The thickness of films was determined by a profilometer and was further confirmed by UV-Visible spectroscopy analysis. Fig. 1 shows variation of film thickness as a function of substrate temperature for CdS films deposited by using RF magnetron sputtering. As seen the CdS film thickness decreases from $1.10 \mu\text{m}$ to $0.26 \mu\text{m}$ when substrate temperature increased from 50°C to 400°C .

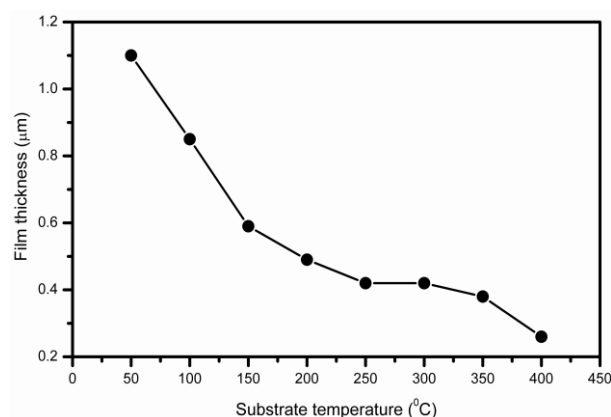


Fig 1 – Variation of film thickness as function of substrate temperature of CdS thin films deposited by RF magnetron sputtering

The decrease in film thickness with increase in substrate temperature can be attributed to the increase in the radical surface mobility of ad-atom at the growing surface. At low substrate temperature, the radical surface mobility of ad-atom is very low and large number of these ad-atoms is incorporated in the growing film. With an increase in substrate temperature each radical receives sufficient energy and its surface mobility en-

hances. This increases their diffusion length allowing them to choose favorable low energy sites. As a result the film thickness decreases with increase in substrate temperature. The decrease in film thickness with increase in substrate temperature was reported previously for CdS films by deposited by spray pyrolysis method [19] and thermal evaporation method [20].

3.2 Low Angle XRD Analysis

Low angle x-ray diffraction (low angle-XRD) is a widely used nondestructive technique for the structural characterization of different materials. Fig. 2 shows XRD pattern of as-deposited CdS films deposited on glass substrate at various substrate temperatures.

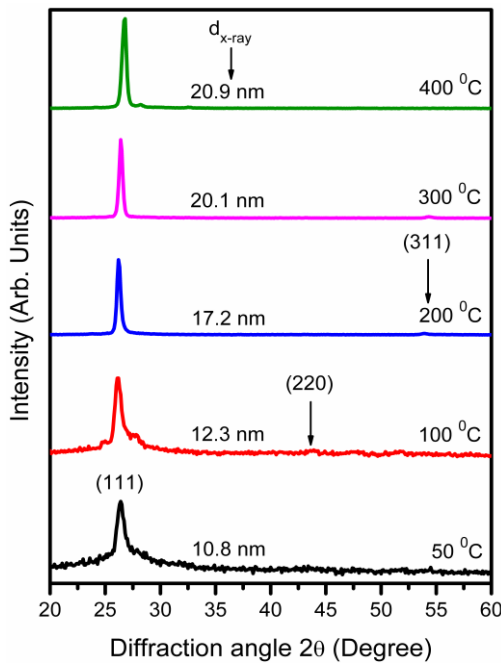


Fig. 2 – Low angle-XRD pattern of CdS films deposited at different substrate temperatures by RF magnetron sputtering

The CdS films deposited at low substrate temperature show one major diffraction peak at $2\theta \sim 26.5^\circ$ and two tiny peaks at $2\theta \sim 43.8^\circ$ and 51.4° corresponding to the (111), (220) and (311) diffraction planes indicating cubic phase of CdS (JCPDS data card No. # 75-1531) suggesting that CdS crystallites have preferred orientation in (111) direction. Significant changes in XRD pattern has been observed in CdS films with increase in substrate temperature. With increase in substrate temperature the line-width (full width at half maximum, FWHM) of diffraction plane (111) decreases and, its sharpness and intensity increases implying increase in its average grain size ($d_{x\text{-ray}}$) and crystallinity. The average crystallite size has been estimated using the classical Scherrer's formula,

$$d_{x\text{-ray}} = \frac{0.9 \lambda}{\beta \cos \theta_B}, \quad (1)$$

where, λ is the wavelength of diffracted radiation, θ_B is the Bragg angle and β is FWHM in radians and its value was found to be in the range $\sim 11\text{-}21$ nm over the

entire range of substrate temperature studied. These values are also shown in Fig. 2. Furthermore, with increase in substrate temperature the diffraction peaks corresponding to (220) and (311) crystallographic planes were found disappeared completely. These results indicate formation of single crystal CdS films with increase in substrate temperature.

3.3 Raman Spectroscopy Analysis

Raman spectroscopy is a very powerful non-destructive technique used to investigate the structure of materials because it gives a fast and simple way to determine the phase of the material, whether it is amorphous, crystalline or nanocrystalline. Fig. 3 shows the Raman spectra of CdS films deposited at different substrate temperatures by using RF magnetron sputtering. The Raman spectra show one major peak centered $\sim 299 \text{ cm}^{-1}$ and another small peak centered $\sim 601 \text{ cm}^{-1}$. They can be assigned to the first and second-order longitudinal optic (LO) phonon modes of CdS, respectively [21]. No marked change in the peak position was observed. No other vibrational modes have been observed over the entire range of substrate temperature studied except a tiny weak peak at $\sim 391 \text{ cm}^{-1}$ which is due to multiple phonon scattering and corresponds to $1\text{LO} + 2\text{E}_2$ phonon mode. These results signify formation of pure CdS phase. These results are consistent with low angle XRD analysis and further confirm the formation of single crystal CdS thin films by RF magnetron sputtering.

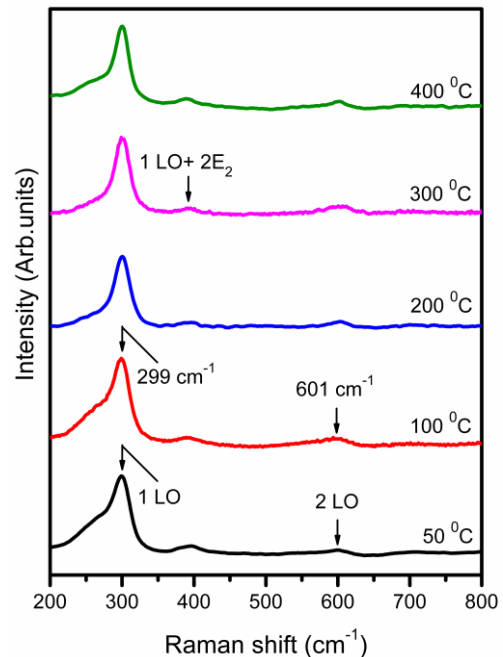


Fig. 3 – Raman spectra of CdS films deposited at different substrate temperatures by RF magnetron sputtering

The ratio of 2LO mode intensity to 1LO mode intensity ($I_{2\text{LO}}/I_{1\text{LO}}$) reflects the exciton-phonon coupling and can be attributed to first an increase of the overlap of the spatial wave functions of the electron and the hole in the electronic excited states in the nanoparticles, and the second due to a big decrease of the lifetime of the ex-

cited state due to trapping on defects on the surface. It has been reported that the ratio I_{2LO}/I_{1LO} depends on crystal phases of CdS where a strong decrease in the I_{2LO}/I_{1LO} ratio was observed for the hexagonal phase and a weaker one was observed for the cubic phase [22]. A large decrease of I_{2LO}/I_{1LO} ratio for nano-particles in comparison with a single crystal has been observed depending on the nanoparticle sizes [23]. In contradiction, Pan et al. [24] found an increase in ratio from bulk CdS to CdS nano-wires having larger dimensions. Recently, Diwate et al. [25] observed increase in I_{2LO}/I_{1LO} with increase in substrate temperature for CdS films deposited by chemical spray pyrolysis and attributed to increase in average grain size of CdS with substrate temperature. In the present study, the ratio, I_{2LO}/I_{1LO} was calculated for the CdS films and was found ~ 0.10 - 0.11 over the entire range of substrate temperature studied. On the other hand, the average grain size increases with increase in substrate temperature (see Fig. 2). These results suggest that for CdS films deposited by RF magnetron sputtering the ratio I_{2LO}/I_{1LO} is independent of average grain size.

3.4 SEM and EDX Analysis

Scanning electron microscopy (SEM) is a convenient method for studying the topography and the growth of CdS thin films. Fig. 4 illustrates the SEM micrographs of CdS thin films grown at different substrate temperatures at $\times 100000$ magnification. All SEM images were taken using a JEOL JSM-6360-LA scanning electron microscope. Before imaging, the samples were coated with platinum by sputter method. All CdS films are highly dense, homogeneous, and free of flaws and cracks. The films show complete coverage over the glass substrates and highly smooth surface indicating that surface morphology of CdS films are independent on substrate temperature. The occurrence of oscillations in UV-Visible transmission spectra further support this conjecture. From SEM images it is clear that the morphological properties of CdS films deposited using RF magnetron sputtering are independent on substrate temperature. Recently, Islam and others [17] also observed quite smooth surface morphology for RF magnetron sputtered CdS thin films compared to CdS thin

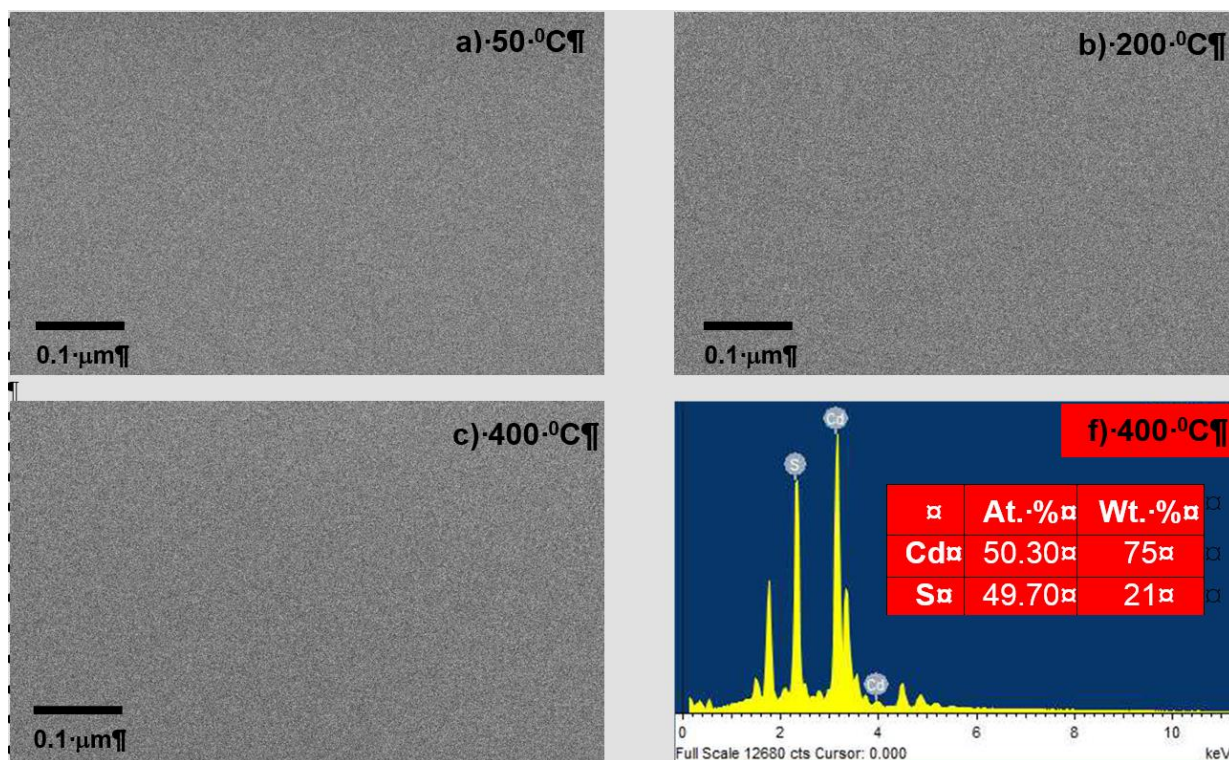


Fig. 4 – Scanning electron microscopy images of CdS thin films grown at different substrate temperatures at $\times 100000$ magnification a) 50 °C, b) 200 °C and c) 400 °C and d) Typical EDX spectra of CdS film deposited at deposition temperature 400 °C

films prepared by using close spaced vapour transport (CSVT) and chemical bath deposition (CBD) methods. The energy-dispersive x-ray (EDX) spectroscopy analysis is an important technique to estimate the chemical composition of the material. Fig. 4(f) shows a typical EDX spectra of CdS film deposited at deposition temperature 400 °C. The results indicate the presence of Cd and S peaks with intensity proportional to their respective concentrations. The EDX results of composition of Cd and S for other CdS films are depicted in Table 2. The films contain mainly Cd and S in atomic % and negligible amount of impurity

indicating the purity of deposited material.

Table 2 – EDX analysis of CdS thin films

Substrate temperature (°C)	Cd (at. %)	S (at. %)	Cd/S ratio
50	49.6	50.3	0.99
100	49.8	50.2	0.99
200	49.8	50.9	0.96
300	50.9	49.1	1.04
400	50.3	48.7	1.03

The EDX data analysis reveals that the atomic ratio of Cd:S is $\sim 1:1$ which confirms the formation of high-quality stoichiometric CdS films by RF magnetron sputtering. It is worth to mentioned that CdS films deposited at low substrate temperatures ($< 200^\circ\text{C}$) are slightly rich in S compare to Cd while deposited at higher temperatures ($> 200^\circ\text{C}$) are slightly Cd rich compare to S.

3.5 UV-Visible Spectroscopy Analysis

The UV-Visible spectroscopy is used to study the optical properties of the CdS thin films deposited at different deposition temperature using RF magnetron sputtering. Figure 5(a) shows the transmission spectra of the CdS thin films deposited at the different substrate temperatures by RF magnetron sputtering in the range 350-800 nm. A sharp absorption edge has been observed in the visible region, indicating good degree of crystallinity and low defect density near the band edge. The presence of interferences fringes in the transmittance spectra indicates that films have smooth surface morphology. The transmission of a film strongly depends on the film structure, which is determined by the preparation methods, film thickness and deposition conditions [26]. Furthermore, the transmittance of films is the result of combination of several effects such as structural homogeneity, better crystallinity and the smooth surface [27]. In the present study the average transmission was found in the range 80-90 % in the visible range which is good for opto-electronic devices, especially buffer layer in CdTe/CdS, Cu₂S/CdS hetero-junction solar cells. As seen from the scanning electron microscopy images the CdS films deposited by RF magnetron sputtering exhibits smooth morphology and XRD analysis reveled that these films are highly crystalline. The presence of smooth morphology and high degree of crystallinity reduces the light scattering. As a result, CdS films show high transmittance in visible range of solar spectrum.

In the direct transition semiconductor, the optical energy band gap (E_{opt}) and the optical absorption coefficient (α) are related by,

$$(\alpha E)^{1/2} = B^{1/2}(E - E_{opt}), \quad (2)$$

where α is the absorption coefficient, B is the optical density of state and E is the photon energy. The absorption coefficient (α) can be calculated from the transmittance of the films with the formula,

$$\alpha = \frac{1}{d} \ln \left(\frac{1}{T} \right), \quad (3)$$

where d is the thickness of the films and T is the transmittance. Therefore, the optical band gap is obtained by extrapolating the tangential line to the photon energy ($E = h\nu$) axis in the plot of $(\alpha h\nu)^2$ as a function of $h\nu$ (Tauc plot). Variation of optical gap as a function of substrate temperature for CdS films deposited by using RF magnetron sputtering method is shown in fig. 5(b) and the inset shows typical Tauc plots for films deposited at 50°C , 200°C and 400°C . As seen the optical band gap increases from 2.28 eV to

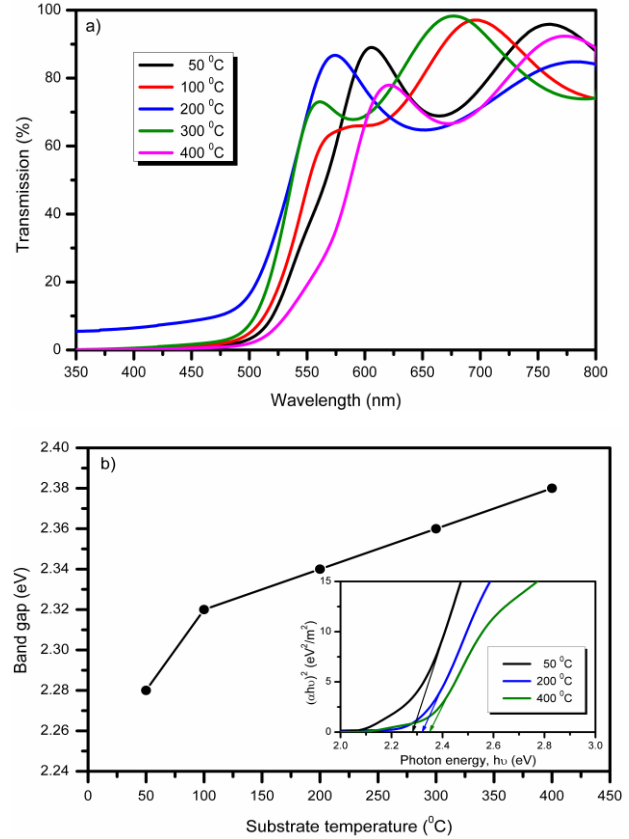


Fig. 5 – Transmission spectra (a) and variation of optical gap as a function of substrate temperature for CdS films deposited by using RF magnetron sputtering method (b). The inset is typical Tauc plots for films deposited at 50°C , 200°C and 400°C

2.38 eV when the substrate temperature increased from 50°C to 400°C .

The increase in band gap with increase in substrate temperature can be attributed to increase in average grain size and increase in crystallinity with substrate temperature. With increase in substrate temperature sharp absorption edge is formed in transmission spectra [see Fig. 5(a)] due to improvement in crystallinity of CdS films and increase in average grain size [see Fig. 2]. These results suggest that the high band gap makes CdS a more effective window material in photovoltaic applications like the CdS/CdTe and CdS/Cu₂S solar cells. Increase in band gap with increase in substrate temperature is well established in the literature for CdS films deposited by chemical spray pyrolysis [28], ultrasonic spray pyrolysis [29] methods.

4. CONCLUSION

Thin films of single crystal CdS were grown by RF magnetron sputtering at various substrate temperatures. Structural, optical and morphology properties of these films was investigated by using various characterization techniques. Formation of single crystal CdS films has been confirmed by low angle XRD and Raman spectroscopy analysis. Low angle XRD showed that CdS films has preferred orientation in (111) direction and increase in substrate temperature improves crystallinity and average grain size in the CdS films. Surface

morphology investigated using SEM showed that CdS films deposited over entire range of substrate temperature are highly smooth, dense, homogeneous, and free of flaws and cracks. The EDX data revealed the formation of high-quality stoichiometric CdS films by RF magnetron sputtering. Furthermore, the CdS films deposited at low substrate temperatures (< 200 °C) are

slightly S rich while deposited at higher substrate temperatures (> 200 °C) are slightly Cd rich. The UV-Visible spectroscopy analysis showed that an average transmission ~ 80 - 90 % in the visible range of the spectrum having band gap ~ 2.28 - 2.38 eV, which is quite close to the optimum value of band gap for a buffer layer in CdTe/CdS, $\text{Cu}_2\text{S}/\text{CdS}$ hetero-junction solar cells.

REFERENCES

1. H. Khallaf, I.O. Oladeji, G. Chai, L. Chow, *Thin Solid Films* **516**, 7306 (2008).
2. Y. Douri, J. Waheb, M. Ameri, R. Khenata, A. Bouhemadou, A. Reshak, *Int. J. Electrochem. Sci.* **8**, 10688 (2013).
3. S.J. Ikhmayies, Ph. D. Thesis, University of Jordan (2002).
4. J. Trajic, M. Gilic, N. Romcevic, M. Romcevic, G. Stanisic, B. Hadzic, M. Petrovic, Y.S. Yahia, *Sci. Sintering* **47**, 145 (2015).
5. M.H Ehsani, H.R. Dizaji, *Chalcogen. Lett.* **8**, 33 (2011).
6. P. Boieriu, R. Sporcken, Y. Xin, N. Browning, S. Sivananthan, *J. Electron. Mater.* **29**, 718 (2000).
7. Y. Guo, J. Jiang, S. Zuo, F. Shi, J. Tao, Z. Hu, X. Hu, G. Hu, P. Yang, J. Chu, *Sol. Energy Mater. Sol. Cells* **178**, 186 (2018).
8. V. Kumar, D.K. Sharma, M.K. Bansal, D.K. Dwivedi, T.P. Sharma, *Sci. Sinter.* **43**, 335 (2011).
9. T.M. Khan, T. BiBi, *SOP Trans. Appl. Phys.* **1**, 48 (2014).
10. Y. Zhang, H. Ma, D. Wu, R. Li, X. Wang, Y. Wang, W. Zhu, Q. Wei, B. Du, *Biosens. Bioelec.* **77**, 936 (2016).
11. W. Kim, M. Baek, K. Yong, *Sens. Actuat. B* **223**, 599 (2016).
12. K. Wilson, M. Ahamed, *Appl. Surf. Sci.* **361**, 277 (2016).
13. S. Yilmaz, Y. Atasoy, M. Tomakin, E. Bacaksız, *Superlat. Microstruct.* **88**, 299 (2015).
14. D. Albin, Y. Yan, D. King, H. Moutinho, K. Jones, *NCPV Prog. Rev. Meet.* **2000**, 289 (2000).
15. D. Barreca, A. Gasparotto, C. Maragno, E. Tondello, *J. Electrochem. Soc.* **151**, G428 (2004).
16. A. Punnoose, M. Marafi, G. Prabu, F.El Akkad, *phys. status solidi a* **177**, 453 (2000).
17. M. Islam, M. Hossain, M. Aliyu, P. Chelvanathan, Q. Huda, M. Karim, K. Sopian, N. Amin, *Energ. Proc.* **33**, 203 (2013).
18. A. Jadhavar, A. Bhorde, V. Waman, H. Pathan, S. Jadkar, *Eng. Sci.* **5**, 126 (2015).
19. A. Ashour, *Turk. J. Phys.* **27**, 551 (2003).
20. S. Jassim, A. Zumail, G. Waly, *Res. in Phys.* **3**, 173 (2013).
21. P. Kumar, N. Saxena, R. Chandra, V. Gupta, A. Agarwal, D. Kanjilal, *Nanoscale Res. Lett.* **7**, 584 (2012).
22. W. Shen, *Physica B* **322**, 201 (2002).
23. R. Kostic, N. Romcevic, *Phys. Stat. Sol. C* **1**, 2646 (2004).
24. A. Pan, R. Liu, Q. Yang, Y. Zhu, G. Yang, B. Zou, K. Chen, *J. Phys. Chem. B* **109**, 24268 (2005).
25. K. Diwate, A. Pawbake, S. Rondiya, R. Kulkarni, R. Waykar, A. Jadhavar, A. Rokade, K. Mohite, M. Shinde, H. Pathan, R. Devan, S. Jadkar, *J. Semicond.* **38**, 023001 (2017).
26. C.S. Tepantlan, A.M. Gonzalez, I.V. Arreola, *Rev. Max. Fis.* **54**, 112 (2008).
27. A. Bouhdjer, A. Attaf, H. Saidi, H. Bendjedidi, Y. Benkhetta, I. Bouhaf, *J. Semicond.* **36**, 082002 (2015).
28. Y. Lee, S. Im, J. Rhee, *Appl. Mater. Interf.* **2**, 1648 (2010).
29. V. Bilgin, S. Kose, F. Atay, I. Akyuz, *Mater. Chem. Phys.* **94**, 103 (2005).